# On the Expansion Rate and Age of the Supernova Remnant G266.2−1.2 (Vela Jr.)

**Allen, G. E.[1], Chow, K.[2], DeLaney, T.[3], Filipović, M. D.[4], Houck, J. C.[5], Pannuti, T. G.[6], Stage, M. D.[7]**

[1]MIT, [2]Weston High School, [3]West Virginia Wesleyan College, [4]Univ. of Western Sydney, [5]Harvard-Smithsonian Center for Astrophysics, [6]Morehead State Univ., [7]Univ. of Massachusetts, Amherst

## 1. Introduction

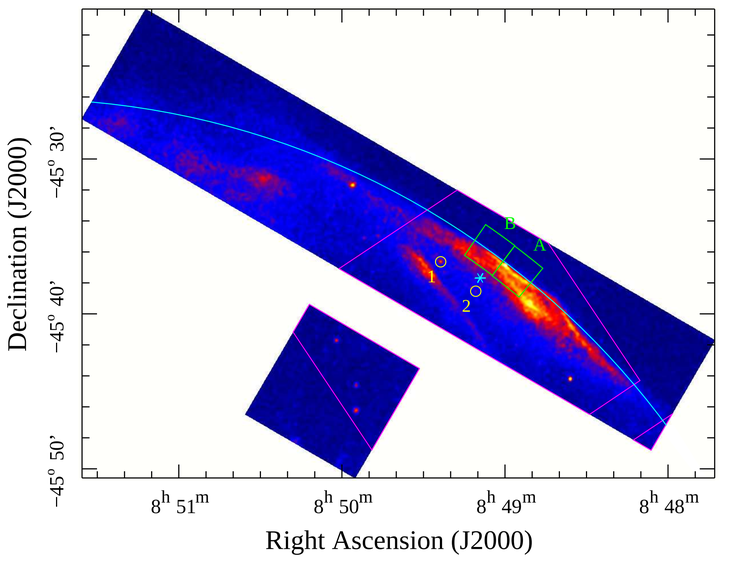


**Figure 1:** *A 1–5 keV image of the northwestern rim of G266.2−1.2 from the 2003 Chandra observation. The cyan asterisk is the location of the aim point. The image has been smoothed using a two-dimensional Gaussian function with $\sigma_X = \sigma_Y = 10$ pixels $= 4.92$ arcsec. The color is a linear function of the flux and varies from about $1 \times 10^{-9}$ or less (dark blue) to $1.4 \times 10^{-8}$ or more (white) in units of photons cm$^{-2}$ s$^{-1}$ pixel$^{-1}$. The magenta lines mark the boundary of the region that was observed in both 2003 and 2008. The yellow circles encompass registration sources 1 and 2. The green annular wedges mark the boundaries of regions A and B, which were used to measure the rate of expansion. The cyan arc is a segment of a circle that has a radius of $0.8642°$ and that is centered on the location of CXOU J085201.4–461753 (Pavlov et al., 2001).*

The shell-type supernova remnant G266.2−1.2 was discovered in the *ROSAT* all-sky survey data and, based upon its equatorial coordinates, named RX J0852.0−4622 (Aschenbach, 1998). To the extent that it is possible to distinguish the emission of G266.2−1.2 from the emission of Vela, the X-ray and radio spectra of G266.2−1.2 appear to be dominated by synchrotron radiation (Slane et al., 2001; Bamba et al., 2005; Stupar et al., 2005; Pannuti et al., 2010). We used the *Chandra* telescope to observe the thin filaments in the bright northwestern region of G266.2−1.2 in 2003 (Fig. 1) and 2008 to measure the rate of expansion of this rim.

## 2. Data and Analysis

Table 1. Expansion results

| Quantity[a] | Region A | Region B |
|---|---|---|
| Region boundaries: | | |
| Radius $\theta$ [deg] | 0.8442–0.8842 | 0.8447–0.8847 |
| Azimuth $\phi$ [deg] | 320.0–322.5 | 322.5–325.0 |
| Model parameters: | | |
| Radial offset $\Delta\theta$ [arcsec] | $1.98 \pm 0.72$ | $3.03 \pm 0.89$ |
| Scale factor $s$ | $0.363 \pm 0.011$ | $0.324 \pm 0.012$ |
| Bkgd 2003 [events arcsec$^{-2}$] | $0.138 \pm 0.003$[b] | $0.127 \pm 0.003$[b] |
| Bkgd 2008 [events arcsec$^{-2}$] | $0.046 \pm 0.002$[b] | $0.042 \pm 0.002$[b] |
| Expansion: | | |
| Time difference $\Delta t$ [yr] | 5.652 | 5.652 |
| $\dot\theta = \Delta\theta/\Delta t$ [arcsec yr$^{-1}$] | $0.35 \pm 0.13$ | $0.54 \pm 0.16$ |
| $\theta$ [deg] | $0.86 \pm 0.17$[c] | $0.86 \pm 0.17$[c] |
| $\dot\theta/\theta$ [kyr$^{-1}$] | $0.113 \pm 0.047$ | $0.172 \pm 0.061$ |

[a] The statistical uncertainties are listed at the 90% conf. level
[b] These values are based upon the sizes of and numbers of events in source free portions of the regions.
[c] A 20% uncertainty in the shock radius is assumed because the location at which the progenitor exploded is unknown.

The data were reprocessed with version 4.6 of the CIAO suite of analysis tools and with version 4.6.1.1 of the CALDB. Our analyses were limited to the energy range from 1–5 keV to minimize the contributions from the Vela supernova remnant and from the charged particle background. Point sources 1 and 2 (see Fig. 1) were used to search for evidence of registration errors, but no such evidence was found. Radial profiles were created for regions A and B (see Fig. 1) using the data for each observation. After compensating for differences in the number of background events, the 2003 profile was shifted by a radial offset $\Delta\theta$, scaled by a factor $s$ (to compensate for differences in the detection efficiencies, observing times, and source fluxes), and compared the the 2008 profile. The offset and scaling parameters were allowed to vary freely in the fit. The best-fit results are listed in Table 1 and plotted in Figures 2 and 3.

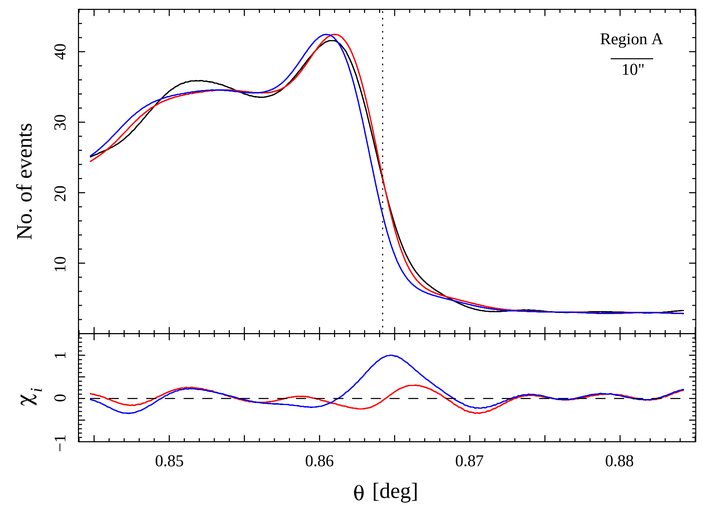


**Figure 2:** *Top panel: Radial profiles for region A (see Fig. 1). The black curve is the number of events in each radial bin from the 2008 dataset. Here, the bins are 1 pixel (0.492 arcsec) wide. The dotted vertical line at $\theta = 0.8642°$ is the radius at which the number of events in 2008 is halfway between the peak of the black curve and the nominal number of background events. The blue and red curves are scaled versions of the 2003 profile before and after, respectively, it has been radially shifted by 2.0 arcsec. Bottom panel: The differences between the black profile and the blue and red profiles divided by the 1-$\sigma$ statistical uncertainties.*

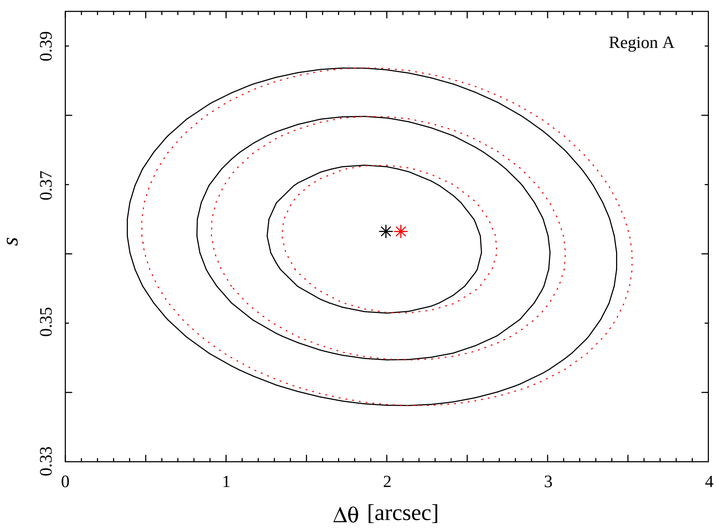


**Figure 3:** *The 1-, 2-, and 3-$\sigma$ confidence contours for region A (see Fig. 1) in the parameter space defined by the radial offset $\Delta\theta$ and the scaling factor $s$. The solid black and dotted red contours are the results obtained before and after, respectively, the mean $\Delta\alpha$ and $\Delta\delta$ registration adjustments are included. The stars indicate the best-fit values of $\Delta\theta$ and $s$. The evidence of expansion in region A (i.e. the evidence that $\Delta\theta > 0$) is significant at nearly the 4-$\sigma$ confidence level.*

The weighted mean offset for regions A and B is $\Delta\theta = 2.40 \pm 0.56$ arcsec. Since the time between the observations is 5.652 yr, the expansion rate $\dot\theta = 0.42 \pm 0.10$ arcsec yr$^{-1}$. This rate is half the rate reported for an analysis of *XMM-Newton* data ($5.5 \pm 1.5$ arcsec over 6.5 yr from 2001 to 2007 or $0.85 \pm 0.23$ arcsec yr$^{-1}$, Katsuda, Tsunemi & Mori, 2008).

## 3. Discussion

To obtain a constraint on the age of G266.2−1.2, we used the hydrodynamic models of Truelove & McKee (1999). Since the physical conditions—the initial kinetic energy ($E_0$), mass ($M_{\rm ej}$), and mass density distribution ($\rho_{\rm ej} \propto v^{-n}t^{-3}$) of the ejecta, the ambient mass density distribution ($\rho_0 = 1.42 m_{\rm p} n_0$), and the evolutionary state ($t/t_{\rm ch}$)—are unknown, a five-dimensional grid in $E_0$, $M_{\rm ej}$, $n$, $n_0$, and $t/t_{\rm ch}$ was used with 81 values of $E_0$: $10^{49}$, $10^{49.05}$, …, $10^{53}$ ergs; 41 values of $M_{\rm ej}$: $10^0$, $10^{0.05}$, …, $10^2$ $M_\odot$; seven values of $n$: 6, 7, 8, 9, 10, 12, 14; 101 values of $n_0$: $10^{-5}$, $10^{-4.95}$, …, $10^0$ cm$^{-3}$; and 999 values of $t/t_{\rm ch}$: 0.01, 0.02, …, 9.99. Of the 2.35 billion scenarios, 57.4 million are consistent with the *Chandra* expansion results, have a shock speed greater than 1000 km s$^{-1}$ (Pannuti et al., 2010; Allen et al., 2008), have a ambient density less than 0.4 cm$^{-3}$ (from an analysis of *ROSAT* data), and do not have an implausibly large inferred cosmic-ray energy. The distribution of the ages of these 57.4 million scenarios is shown in Figure 4. If the *Chandra* expansion rate for the northwestern rim is representative of the remnant as a whole, then the age is most likely between 2.4 and 5.1 kyr. Even if G266.2−1.2 is expanding into a steady stellar wind instead of a uniform ambient medium, the age is not expected to increase by more than a factor of 1.5. In the unlikely case that G266.2−1.2 was produced by a Type Ia event, the expected age range is within the range shown in Figure 4.

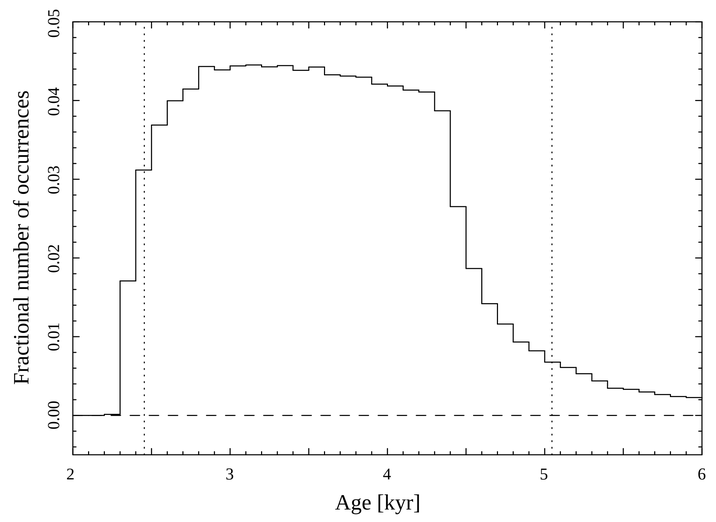


**Figure 4:** *The distribution of the ages of the 57.4 million plausible hydrodynamic scenarios. No age is less than 2.2 kyr or greater than 8.4 kyr. If the lowest 5% and highest 5% of the distribution are ignored, then the plausible ages lie between about 2.4 and 5.1 kyr (i.e. between the dotted vertical lines).*

The hydrodynamic analysis does not provide a significant constraint on the distance. An analysis of previously-published distance estimates and constraints suggests that the remnant is between about 0.5 and 1.0 kpc (Allen et al., 2014). We adopt the distance of the closer of two groups of material in the Vela Molecular Ridge (i.e. $0.7 \pm 0.2$ kpc, Liseau et al., 1992) as the distance of the remnant. This distance is consistent with the progenitor having been a member of the Vel OB1 association (Eggen, 1982).

## 4. Conclusions

- An analysis of the data for two *Chandra* observations of G266.2−1.2 indicates that it has expanded by $2.40 \pm 0.56$ arcsec over a period of 5.652 yr (i.e. by $0.42 \pm 0.10$ arcsec yr$^{-1}$ or about half the rate reported by Katsuda, Tsunemi & Mori (2008)).
- The results of a hydrodynamic analysis suggest the remnant is most likely between about 2.4 and 5.1 kyr old whether it was produced by a Type II or Type Ia event. The age could be up to a factor of 1.5 larger if G266.2−1.2 is expanding into a steady stellar wind instead of a uniform ambient medium. In no case is the age expected to be less than 2.2 kyr. Therefore, G266.2−1.2 is too old to be associated with emission from the decay chain of $^{44}$Ti.

## 5. Acknowledgements

G.E.A. is supported by contract SV3-73016 between MIT and the Smithsonian Astrophysical Observatory. The Smithsonian Astrophysical Observatory is operated on behalf of NASA under contract NAS8-03060. This research has made use of data products from the Chandra Data Archive, the Two Micron All Sky Survey, and the USNO-B1.0 catalog. The analyses described herein were performed using the software package CIAO, provided by the Chandra X-ray Center, the software package ISIS (Houck & Denicola, 2000), the scripting language S-Lang, and the models of the XSPEC spectral-fitting package.

## References

Allen, G. E., Houck, J. C., & Sturner, S. J. 2008, ApJ, 683, 773

Allen, G. E., et al. 2014, ApJ, accepted (http://arxiv.org/abs/1410.7435)

Aschenbach, B. 1998, Nature, 396, 141

Aharonian, F., et al. 2005, A&A, 437, L7

Bamba, A., Yamazaki, R., & Hiraga, J. S. 2005, ApJ, 632, 294

Eggen, O. J. 1982, ApJS, 50, 199

Houck, J. C., & Denicola, L. A. 2000, in ASP Conf. Ser. 216, Astronomical Data Analysis Software and Systems IX, ed. N. Manset, C. Veillet, & D. Crabtree, 591

Katsuda, S. Tsunemi, H., & Mori, K. 2008, ApJ, 678, L35

Liseau, R., et al. 1992, A&A, 265, 577

Pannuti, T. G., et al. 2010, ApJ, 721, 1492

Pavlov, G. G., et al. 2001, ApJ, 559, L131

Slane, P., et al. 2001, ApJ, 548, 814

Stupar, M., et al. 2005, Adv. Space Res., 35, 1047

Truelove, J. K. & McKee, C. F. 1999, ApJS, 120, 299